

# Electron Cloud Modeling for the ILC Damping Rings

J.A. Crittenden, D.C. Sagan and K.G. Sonnad  
CLASSE\*, Cornell University, Ithaca, NY 14850, USA

## Abstract

Electron cloud buildup is a primary concern for the performance of the damping rings under development for the International Linear Collider. We have performed synchrotron radiation rate calculations for the recent 3.2-km DSB3.2 lattice design using the SYNRAD utility in the Bmad accelerator software library. These results are then used to supply input parameters to the electron cloud modeling package ECLOUD. Contributions to coherent tune shifts from the field-free sections, and from the dipole and quadrupole magnets have been calculated, as well as the effect of installing solenoid windings in the field-free regions. For each element type, SYNRAD provides ring occupancy, average beam sizes, beta function values, and beta-weighted photon rates for the coherent tune shift calculation. An approximation to the antechamber design has been implemented in ECLOUD as well, moving the photoelectron source points to the edges of the antechamber entrance and removing cloud particles which enter the antechamber.

## INTRODUCTION

The International Linear Collider (ILC) Damping Rings Working Group has undertaken a broad-based effort to quantify operational limits arising from electron cloud buildup for various lattice designs with the goal of establishing recommendations for mitigation techniques [1]. The ECLOUD [2] and POSINST [3] cloud buildup modeling programs have been adapted to describe measurements of coherent tune shifts in the context of the Cornell Electron Storage Ring Test Accelerator (CesrTA) program [4] providing stringent constraints on input parameters for a wide variety of beam energies, bunch patterns and bunch current levels [5, 6, 7]. We describe work applying the modeling methods used for CesrTA to the recent ILC DSB3.2 lattice damping ring design [8]. The synchrotron radiation analysis utility SYNRAD, implemented in the Bmad program package [9], is used to provide photon rates, beam sizes and beta functions on an element-by-element basis, as described in the next section.

## SYNCHROTRON RADIATION ANALYSIS

Figure 1 shows the photon rate ( $\gamma/\text{m}/\text{beam particle/turn}$ ) incident on the outside wall of the vacuum chamber as calculated by the SYNRAD utility for the DSB3.2 lattice. The

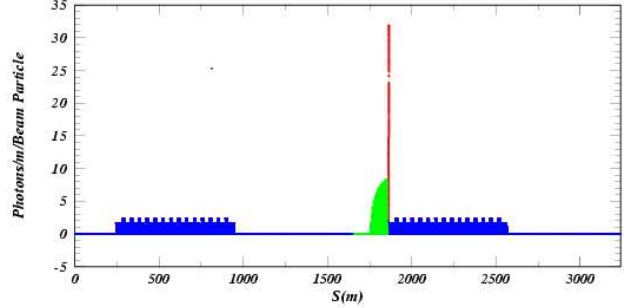


Figure 1: Photon rate ( $\gamma/\text{m}/\text{beam particle/turn}$ ) on the outside wall of the vacuum chamber around the DSB3.2 lattice calculated by the Bmad utility SYNRAD. The rates in the field-free regions are shown in blue, those in the dipoles in red, and those in wigglers in green.

highest rates occur in the dipole magnets downstream of the wigglers. For the purposes of the tune shift calculations described below, we assume that this radiation is either removed or masked and does not contribute. The singular high rate near  $s = 800$  m is a consequence of a reduction in the beam pipe diameter from 2.5 cm to 2.3 cm over a 140-m distance at the end of the first arc, which is the only change in the beam pipe around the ring in this simple model for the vacuum chamber profile. The critical energy of the radiation ranges from 4.6 keV and 6.4 keV for the two dipole strengths in the arcs to 32 keV for the wiggler radiation.

Figure 2 shows the photon rate over a 50-m region at the end of the second arc ( $2500 < s < 2550$  m), illustrating the characteristic of the 3.2-km lattice that the dipoles shine into downstream dipoles, which was not the case in the earlier 6.4-km design. Since the electron cloud buildup

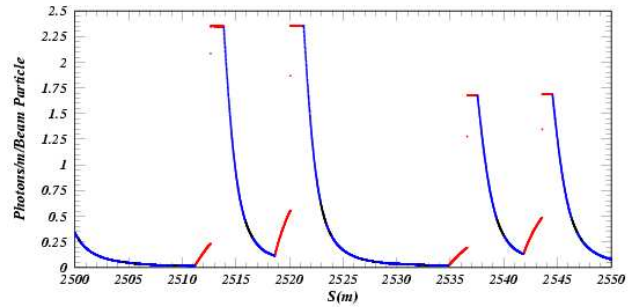


Figure 2: Photon rate over a 50-m region near the end of the second arc on the outside wall of the vacuum chamber, illustrating the characteristic of the 3.2-km lattice design that radiation from the dipoles strike the wall in downstream dipoles.

\*Work supported by the U.S. National Science Foundation PHY-0734867 and the US Department of Energy DE-FC02-08ER41538

Element	Tot Length [m]	Ring Fraction	<Beta X> [m]	<Beta Y> [m]	<Sig X> [mm]	<Sig Y> [mm]	<Photon Rate> [Phot/m/e]	
							Outside	Inside
Dipole	324.2	10.0%	3.6	18.6	0.1207	0.0166	1.083	0.000
Drift	2560.8	79.1%	33.3	31.8	0.2269	0.0210	0.145	0.027
Wiggler	101.9	3.1%	10.8	14.1	0.0899	0.0145	0.729	0.719
Quadrupole	206.8	6.4%	21.5	23.4	0.2897	0.0177	0.236	0.067
Sextupole	44.3	1.4%	20.7	25.3	0.4207	0.0191	0.129	0.000
Non-dipole	2913.8	90.0%	31.5	30.5	0.2295	0.0205	0.171	0.053
Non-drift	677.2	20.9%	11.3	19.8	0.1873	0.0168	0.709	0.129
Total	3238.1	100.0%	28.7	29.3	0.2186	0.0201	0.263	0.048

Table 1: Element-type-specific ring lengths, and averages of beta functions, beam sizes, and photon rates on the outside and inside walls of the vacuum chamber for the DSB3\_2 ILC damping ring lattice design

proceeds very differently in drift regions and dipole fields, such a characteristic affects the coherent tune shifts and the potential for instabilities. In general, cloud buildup in dipoles is more sensitive to the reflection qualities of the vacuum chamber, since photoelectrons produced in the vertical plane containing the beam are trapped on the field lines and remain in the beam region. The central beam density then depends strongly on bunch current, since the strengths of the beam kicks change the energy region of the secondary yield curve which is sampled.

Table 1 shows the element-type-specific ring fraction, beta functions, beam sizes and photon rates used as input to the ECLLOUD electron cloud buildup model. As a consequence of the more compact design of the 3.2-km lattice, the average rate in the dipoles is a factor of three higher than in the 6.4-km lattice. However, the low horizontal beta function will offset the higher rate in the calculation of horizontal tune shifts.

## CALCULATIONS OF COHERENT TUNE SHIFTS

The time-sliced macroparticle-tracking algorithm implemented in the ECLLOUD program accounts for electrostatic forces from the beam bunches and space-charge forces of the cloud, as well as for a variety of choices of magnetic field profiles. Cloud macroparticles are produced and tracked in three dimensions along a 1-m length of vacuum chamber. The beam kicks and space-charge forces are modeled as two-dimensional. Our calculations assess contributions to the coherent tune shift from field-free regions, dipoles (0.27 T), and quadrupoles (7 T/m), as well as estimating the effect of turning on 40-Gauss cloud-mitigating solenoidal magnetic fields in the drift regions. The tune shift magnitudes along the bunch trains are derived from the horizontal and vertical space-charge field gradients calculated at the center of the vacuum chamber immediately prior to the passage of each bunch. The gradients are weighted with the ring fraction and beta functions to obtain the tune shifts. Four trains of 45 bunches were modeled, with a bunch population of  $2.1 \times 10^{10}$  positrons, spaced by 1.8 m. The trains were separated by 27 m. The beam

sizes were chosen to be the element-type averages given by the SYNRAD calculation (see Table 1), corresponding to horizontal and vertical emittances of 750 pm and 2 pm. The bunch length was 5.6 mm. An antechamber opening of  $\pm 5$  mm was assumed to prevent 90% of the incident radiation from producing photoelectrons. The 80% of the photoelectrons were generated along 1-mm-high stripes adjacent to the antechamber opening, the remainder distributed uniformly in azimuth outside of the antechamber region. Particles entering the opening during cloud development were removed from the cloud. However, the boundary conditions applied to the electric field calculations did not account for the antechamber opening. The secondary yield model for electrons hitting the vacuum chamber wall assumed a peak true secondary yield value of 1.2 at a peak energy of 300 eV, a rediffused yield of 0.2, and an elastic yield value of 0.5.

Figure 3 shows the contributions to coherent tune shifts from the drift and dipole regions and their sum. The dipole contribution is negligible. The drift contribution exhibits saturation along the 45-bunch trains, reaching a level of 0.1 kHz and 0.25 kHz for the horizontal and vertical tunes, which can be compared to the horizontal and vertical fractional design tunes of 17.5 kHz and 22.3 kHz.

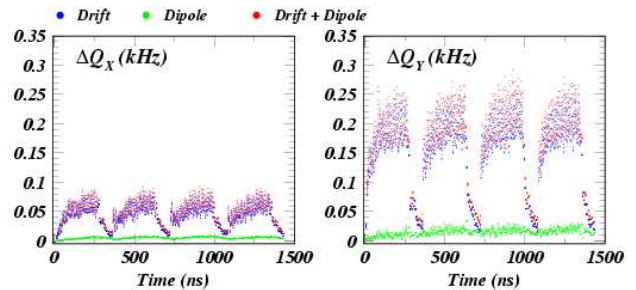


Figure 3: Contributions to coherent tune shifts from the field-free and dipole regions of the DSB\_2 lattice for four 45-bunch trains, each bunch consisting of  $2.1 \times 10^{10}$  positrons. The horizontal and vertical tune shifts of 0.1 kHz and 0.25 kHz can be compared to the horizontal and vertical fractional design tunes of 17.5 kHz and 22.3 kHz.

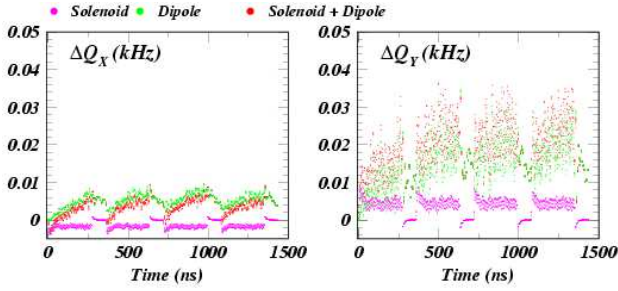


Figure 4: Tune shift calculations showing the effect of turning on 40-Gauss solenoidal magnetic field windings in the drift regions, which effectively removes their contribution to the overall tune shifts.

Figure 4 shows the effect of turning on a 40-Gauss solenoidal magnetic field in the drift regions. Their contribution is effectively eliminated, in fact they slightly compensate the dipole contribution to the horizontal tune shift. The combined tune shifts are reduced to 0.01 kHz and 0.035 kHz.

The quadrupole contributions to the tune shifts were found to be about a factor of two smaller than the dipole contributions, thus not imposing a significant additional operational constraint. It should be noted, however, that this analysis does not account for turn-to-turn cloud trapping in the quadrupoles.

We estimated the effect of the vacuum chamber surface mitigation method by raising the true secondary yield value from 1.2 to 1.8, the value which successfully reproduced the tune shift magnitudes measured at CEsrTA for an uncoated aluminum chamber. The horizontal and vertical tune shifts were found to reach values near 1 kHz along the 45-bunch train, with comparable contributions from drift and dipole regions. The results are shown in Fig. 5.

## SUMMARY

We have applied the modeling analysis technique developed in the context of the CEsrTA program for estimating coherent tune shifts induced by the buildup of electron clouds in the ILC damping rings. The synchrotron radiation characteristics of the recent DSB3.2 lattice de-

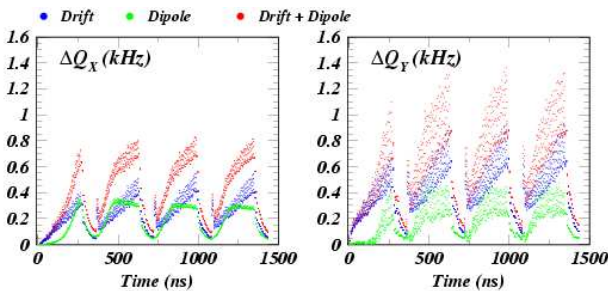


Figure 5: Tune shift calculations for the case of a high true secondary yield value of 1.8, such as was found to reproduce the CEsrTA tune shift measurements, where the vacuum chamber surface is uncoated aluminum.

sign have been calculated and applied as input to the cloud buildup code ECLOUD, allowing the calculation of contributions to the coherent tune shifts from field-free, dipole, and quadrupole regions of the ring, as well as the effect of adding 40-Gauss solenoidal magnetic field windings to the drift regions. The tune shifts are found to arise primarily in the drift regions, reaching 1% of the fractional tune under the assumption of a total secondary yield value of 1.4. The mitigating effect of the solenoids reduces the contribution from the drift regions such that the dipole regions then dominate, and the combined tune shifts are reduced by an order of magnitude. The contribution from the 6% of the ring occupied by quadrupole magnets is calculated to be less than half that from the dipole regions. It should be noted however, that this analysis does not account for cloud electrons trapped in the quadrupoles from turn to turn. Raising the value assumed for the secondary yield to 2.0, a value typical of an uncoated aluminum vacuum chamber, results in solenoid-off tune shift estimates reaching 5% of the fractional tune.

Future work includes incorporating a more detailed model of the vacuum chamber profile. The three-dimensional photon tracking code SYNRAD3D now implemented in Bmad and in use for modeling the CEsrTA measurements [7, 10] will provide estimates of the mitigating effect of the antechamber on photon rates and azimuthal impact distributions. We also plan to employ finite-element electrostatics calculations to account for the boundary conditions of more complicated vacuum chamber profiles such as those including an antechamber.

## REFERENCES

- [1] See contributions by M. Furman, M.T.F. Pivi, and L. Wang, 49th ICFA Advanced Beam Dynamics Workshop, October 8-12, 2010, Cornell University, Ithaca, NY 14853
- [2] F. Zimmermann and G. Rumolo, ICFA Beam Dynamics Newsletter No. 33, eds. K. Ohmi and M.A. Furman (2004)
- [3] M.A. Furman and M.T.F. Pivi, Phys Rev ST-AB 5, 124404 (2002)
- [4] G.F. Dugan, M.A. Palmer, and D.L. Rubin, ICFA Beam Dynamics Newsletter No. 50, eds. J. Urakawa and W. Chou (2009)
- [5] J.A. Crittenden *et al.*, FR5RFP044, PAC09, 4-8 May 2009, Vancouver, British Columbia, Canada
- [6] J.A. Crittenden *et al.*, TUPD024, IPAC10, 23-28 May, 2010, Kyoto, Japan
- [7] D.L. Kreinick *et al.*, WEP108, these proceedings
- [8] S. Guiducci, 2011 Linear Collider Workshop of the Americas (ALCPG11), March 19-23, 2011, Eugene, Oregon 97403
- [9] D. Sagan, *Bmad: A Relativistic Charged Particle Simulation Library*, Nucl. Instrum. & Methods **A558**, 356 (2006). The Bmad manual can be obtained at <http://www.lepp.cornell.edu/~dcs>
- [10] G.F. Dugan, S. Milashuk and D.C. Sagan, 49th ICFA Advanced Beam Dynamics Workshop, October 8-12, 2010, Cornell University, Ithaca, NY 14853